Pergamon

Cement and Concrete Research 33 (2003) 47–53

CEMENT AND CONCRETE RESEARCH

A vacuum-air permeability test for in situ assessment of cover concrete

Peter A. Claisse*, Esmaiel Ganjian, Tarek A. Adham

School of the Built Environment, Coventry University, Priory Street, Coventry CV1 5FB, UK

Received 24 January 2000; accepted 1 July 2002

Abstract

The transport properties of fluids in the cover layer are the main indicator of the durability of reinforced concrete structures. Many laboratory tests exist for measuring these properties. However, there are relatively few tests that can be used on site. In this paper, the development of a new nondestructive rapid test capable of measuring the air permeability of in situ concrete is described. The new method measures the movement of gas between different holes drilled into the concrete and gives results for the permeability of the concrete and for the volume of concrete that has been tested. A pressure measuring method was developed to measure the pressure inside the concrete by using a piezoresistive pressure transducer and a data logger. Four different techniques were investigated and one preparation technique is recommended for in situ use.

Keywords: Degradation; Durability; Long-term performance; Permeability; Transport properties

1. Introduction

1.1. Background

The surface skin of concrete is the first line of defence against the ingress of aggressive agents such as chlorides, sulphates and carbon dioxide. For this reason, there is an increasing awareness of its importance for durability of concrete [1–3].

The problem of durability of concrete usually involves movement of aggressive fluids from the surrounding environment into the concrete through the cover concrete followed by physical and/or chemical action in its internal structure, leading to deterioration. The mechanisms of ingress of harmful materials involved are in fluid form or dissolved in water [4,5].

The main agencies of deterioration of concrete require the presence and movement of water through the material [6,7]. A number of different permeation tests described in the literature (e.g., ISAT, Figg permeation method, CAT and Autoclam) [8–11]. This paper describes the development of a new test that is proposed as an improvement to the Figg method.

1.2. Drilled hole tests in concrete

The measurement of transport to or from a drilled hole is the alternative to surface measurements for in situ assessment of concrete durability [12]. A convenient way of carrying out these tests is to drill a hole, seal the top of it, evacuate the space below the seal and measure the time taken for the vacuum to decay. This is the basis of the Figg test [9]. The problem of moisture in the concrete affecting the test results may be overcome by vacuum drying prior to the test [12]. The test is well established and has been shown to give a good measure of the relative performance of different mixes, but it has been shown [12] that it cannot give any indication of the volume of concrete that it is testing. The Figg test also cannot be used to calculate values of concrete permeability. In order to overcome these difficulties, a new test, which uses additional holes in the concrete, is proposed. In this paper, a number of different methods that were assessed for the new test are compared and results from the test are reported.

The new test is shown in Fig. 1.

2. Theoretical analysis

The volume of concrete that is being tested is measured by the distance X at which the pressure returns to

* Corresponding author. Tel./fax: +44-24-7688-8485.
E-mail address: cbx054@coventry.ac.uk (P.A. Claisse).

0008-8846/03/$ – see front matter © 2003 Elsevier Science Ltd. All rights reserved.
PII: S0008-8846(02)00912-2

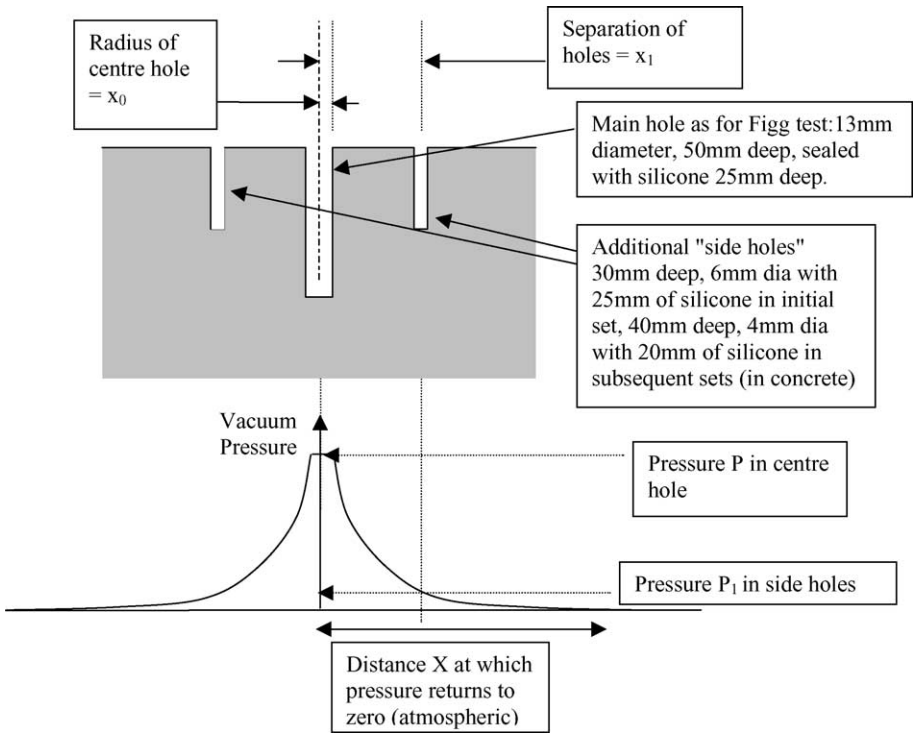

Fig. 1. The drilled hole test.

atmospheric. To calculate this, the steady state is considered in which a constant vacuum is applied to the centre hole.

The modelling is based on the Darcy equation for pressure-driven flow [13]

$$F = \frac{KA}{E}\frac{\mathrm{d}p}{\mathrm{d}x} \tag{1}$$

where F is the flow rate (m^3/s), K is the intrinsic permeability (m^2), E is the viscosity of the fluid (Pa s), p is the pressure (Pa) at a distance x (m) from the high pressure reservoir and A is the area (m^2) across which the fluid is flowing.

In this test, the permeating fluid is compressible and the observed flux F (m^3/s) will therefore change with pressure. The flow is therefore best expressed as molecular flow where N is the total flux (mol m^{-2} s^{-1}) and dn/dt is the flow rate of the gas (mol/s). Both N and dn/dt are approximately constant across the sample (assuming a steady state within it) [12].

$$N = \frac{1}{A}\frac{\mathrm{d}n}{\mathrm{d}t} = -\frac{Kp}{RTE}\frac{\mathrm{d}p}{\mathrm{d}x} \tag{2}$$

where R is the gas constant (8.31 J mol^{-1} K^{-1}), T is the temperature (K) and t is the time from the start of the test (s).

Considering the radial flow into the curved surface of the drilled hole, the area $A = 2\pi xl$.where l is the length of the evacuated volume (m).Eq. (2) therefore becomes:

$$\frac{1}{2\pi l}\int \frac{\mathrm{d}n}{\mathrm{d}t}\frac{\mathrm{d}x}{x} = \frac{K}{RTE}\int P\mathrm{d}p. \tag{3}$$

This flow passes through the region in which the side holes are located.

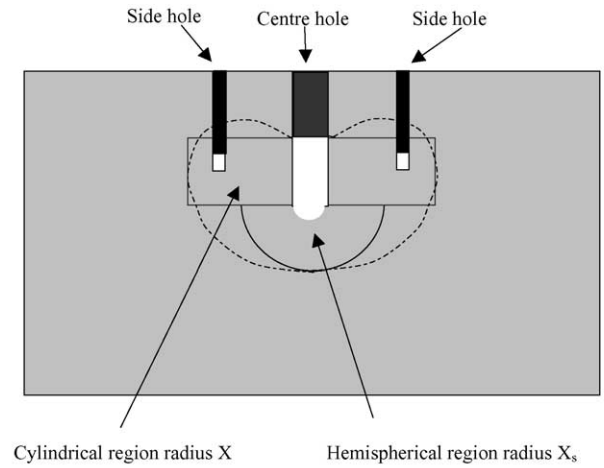

Fig. 2. The developed model for the vacuum decay test.

Table 1
Mortar mix design

Constituent materials (kg/m^3)			w/c
OPC	Water	Sand	
350	245	1400	0.7

Table 2
Concrete mix design

Mix number	Cement (kg/m^3)	Water (kg/m^3)	Coarse aggregate 20 mm (kg/m^3)	Sand (kg/m^3)	w/c
1	395	225	800	980	0.57
2	520	240	1050	590	0.46
3	410	250	1100	625	0.61

Integrating from $X \rightarrow x_1$ where X is the distance from the centre of the main hole to a point where the pressure is atmospheric (m) and x_1 is the distance from the centre of the main hole to the centre of the side hole (m),

$$\frac{dn}{dt}\ln\left(\frac{X}{x_1}\right) = \frac{K}{RTE}(P_a^2 - P_1^2) \quad (4)$$

where P_a is the atmospheric pressure (Pa) and P_1 is the pressure at the side hole (Pa), integrating from $x_1 \rightarrow x_0$ where x_0 is the radius of the main hole (m),

$$\frac{dn}{dt}\ln\left(\frac{x_1}{x_0}\right) = \frac{K}{RTE}(P_1^2 - P^2) \quad (5)$$

where P is the pressure at the main hole (Pa).

Dividing Eq. (4) by Eq. (5) gives:

$$\frac{\ln(X/x_1)}{\ln(x_1/x_0)} = \frac{(P_a^2 - P_1^2)}{(P_1^2 - P^2)}. \quad (6)$$

Eq. (6) may be used to calculate X from experimental observations of P_1.

The intrinsic permeability is obtained from an analysis of the decay transient when the Figg test is applied in the normal way, i.e., a vacuum is applied to the centre hole and then the inlet is sealed and the vacuum decays. An initial analysis of this has been published by the authors [12] and the result is in Eq. (7). It may be seen that the distance X must be known in order to calculate the permeability K.

$$\frac{(P + P_a)(P_i - P_a)}{(P - P_a)(P_i + P_a)} = \exp\left[\frac{2KP_a t}{Ex_0^2 \ln(X/x_0)}\right] \quad (7)$$

When analysing the transient, however, the total flow into the centre hole must be considered. The above analysis takes no account of the flow into the base of the drilled hole. To improve the approximation a second region has been added to the model to include flow into the base of the hole as shown in Fig. 2. The drill bit used produced an approximately hemispherical inner surface to this region.

By including the hemispherical area and following through the integration, Eq. (7) becomes

$$\frac{(P + P_a)(P_i - P_a)}{(P - P_a)(P_i + P_a)} = \exp\left\{\left[\frac{2KP_a t}{Ex_0^2}\right]\left[\frac{1}{\ln\left(\frac{X}{x_0}\right)} - \frac{1}{L\left(\frac{1}{X_s} - \frac{1}{x_0}\right)}\right]\right\} \quad (8)$$

where X_s is the radius of the hemispherical region below the base of the hole and L is the length of the evacuated volume.

Table 3
The methods for preparing the side hole

Method number	Method	Comments
1	6-mm plastic pipes cast in wet concrete; metal rods inside the pipes to keep them clear	cannot be used on existing structures
2	hole drilled in set concrete and filled with epoxy; plastic pipe inserted into wet epoxy; hole drilled through to the concrete when the epoxy had set	
3	hole drilled in set concrete; plastic pipe set into hole with liquid silicon rubber; sponge to keep silicon out of pipe	difficult to inject the silicon to full depth
4	silicon rubber placed in hole to 25 mm depth; hypodermic needle inserted through set silicon	this is the standard Figg method this method selected for the investigation

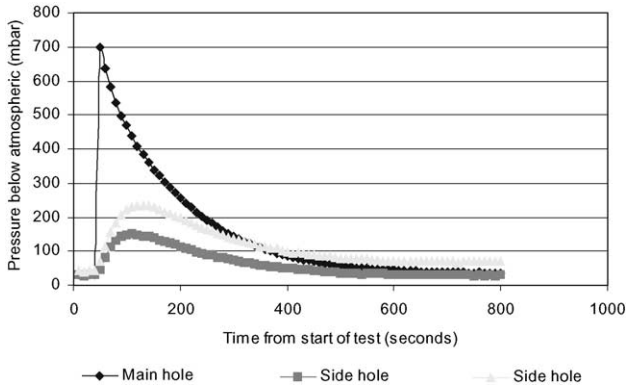

Fig. 3. Pressure decay curves for Method 1 (pipe cast into concrete).

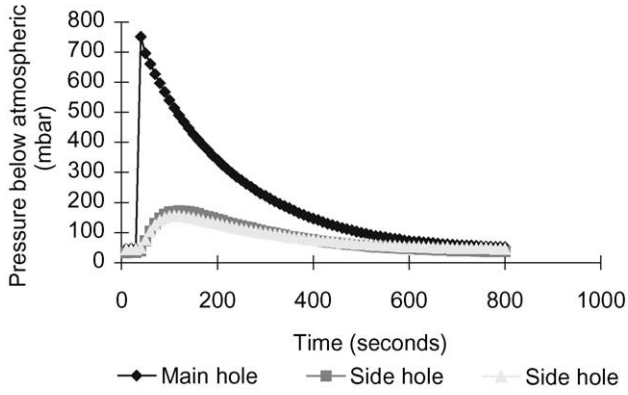

Fig. 4. Pressure decay curves for Method 2 (epoxy seal).

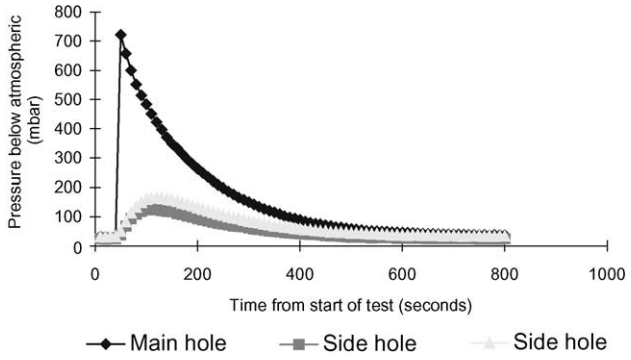

Fig. 5. Pressure decay curves for Method 3 (silicon rubber seal around pipe).

In order to estimate X_s, the authors suggest that it is best to assume that the flow rate (N) per unit area at the boundaries of the two regions is the same.

Equating the two flow rates and solving the equations gives:

$$-X\ln\left(\frac{X}{x_0}\right) = X_s - \frac{X_s^2}{x_0}. \quad (9)$$

Eq. (9) may be used to calculate values of X_s from measured values of X (from Eq. (6)) and these may then be used in Eq. (8) to calculate the permeability. Trial calculations using these equations have indicated that X_s is approximately $0.5X$ and approximately 30% of the flow into the hole comes from the hemispherical region.

3. Casting and curing of specimens

3.1. Mortar mixes

Mortar mixes were made by using a linear horizontal pan type mixer of 0.04 m^3 capacity throughout the study. The mixing of mortar was done according to BS 5075 [14]. The mix design is shown in Table 1.

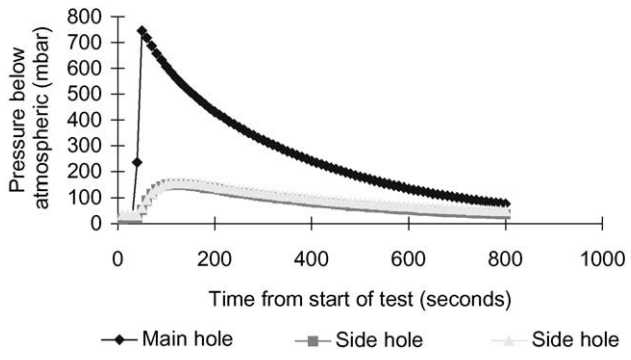

Fig. 6. Pressure decay curves for Method 4 (hypodermic through silicon rubber).

All the samples were cured in water at 20 °C for 7 days and then oven-dried at 105 °C to constant weight and kept in the laboratory until tested.

3.2. Concrete mixes

Three different concrete mixes were designed and made as shown in Table 2.

Three different mould sizes (i.e., 100-mm cube, 150-mm cube and a prism of $400 \times 400 \times 100$ mm) were cast for each concrete mix. All the specimens were air-cured at laboratory temperature for 28 days until tested.

4. Investigation of methods

4.1. The different methods

The new test requires the measurement of pressure in the 'side holes'. These holes are different from the centre hole in that they are only used for measuring pressure (not applying it) and their diameter is as small as possible to prevent disturbance of the pressure decay. Tests were therefore carried out to see if the method of preparing the holes should be different from the normal method for the Figg test that was used on the centre hole.

The four methods for preparing the holes are given in Table 3.

4.2. Experimental procedure

Pressure measurements were made using piezoresistive pressure transducers and a data logger. The different methods were tested by applying a vacuum to the centre hole and then sealing it and letting the vacuum decay. One hundred-millimeter mortar cubes were used with a standard centre hole (13×50 mm, diameter $\times$ depth). The side holes were 6 mm in diameter and 30 mm deep with a 5-mm deep void space. This diameter would be insufficient for measurement of flow rates because a significant proportion of the surface of the void could be obstructed by a single aggregate particle. These holes

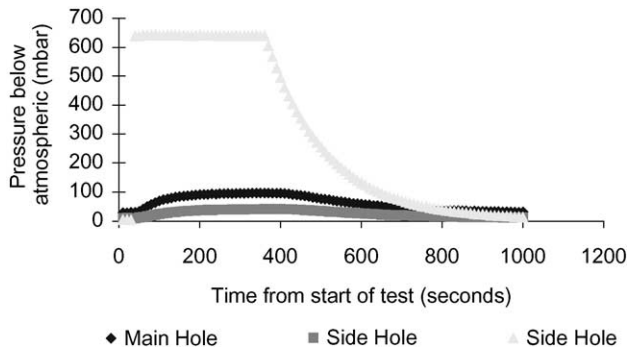

Fig. 7. Pressure curves for a concrete specimen using the new method.

Table 4
Results

Mix no.	w/c	Sample size (mm)	Distance, x_1 (mm)	Pressure, P, at main hole (mm Hg of vacuum)	Pressure, P_1, at side hole (mm Hg of vacuum)	X (mm)	Pressure, P, at main hole (mm Hg of vacuum)	Pressure, P_1, at side hole (mm Hg of vacuum)	X (mm)
1	0.57	100 × 100	30	742	57	38.7	633	56	38.9
		100 × 100	40	742	33	47.2	633	32	47.3
		150 × 150	30	770	117	54.6	656	110	53
		150 × 150	40	770	31	46.8	656	30	46.7
		400 × 400	30	755	158	73.9	640	149	70.9
		400 × 400	40	755	32	46.9	640	31	46.9
2	0.46	100 × 100	30	760	85	44.9	652	83	44.9
		100 × 100	40	760	31	46.7	652	30	46.7
		150 × 150	30	760	92	46.8	646	90	46.9
		150 × 150	40	760	53	52.9	646	52	52.9
		400 × 400	30	736	110	52.2	650	100	49.8
		400 × 400	40	736	81	62.9	650	55	53.9
3	0.61	100 × 100	30	749	129	59.2	636	120	57.2
		100 × 100	40	749	34	47.5	636	15	43.1
		150 × 150	30	745	127	58.4	633	116	55.6
		150 × 150	40	745	55	53.5	633	51	52.7
		400 × 400	30	756	104	50.2	640	98	49.3
		400 × 400	40	756	45	50.5	640	42	49.9

are, however, only used for observation of pressure and the risk of the entire surface of the void being sealed by an uncracked aggregate particle is not seen as significant. A larger hole could cause significant disturbance to the airflow.

4.3. Selection of experimental method

The graph of pressure against time for each preparation technique is presented in Figs. 3–6. Comparison of the graphs of the four preparation techniques reveals that all the pressure decay curves for the different techniques were almost the same. This gives considerable confidence in all of the methods used and indicates that a selection may be made based on practical considerations.

Method 4 is ideal for use on site because Method 1 cannot be used on site and Method 2 is much more time-consuming than Method 4. In Method 3, it is difficult to inject the liquid silicon where the flexible tube limits the remaining space. This action also limits the diameter of the side hole in this technique.

For these reasons the selected technique is Method 4, i.e., drill a hole, fill it with silicon and insert the hypodermic needle.

5. Determination of pressure decay profile

5.1. Experimental procedure

The distance X at which the pressure returns to atmospheric was determined by applying a constant pressure to the centre hole and measuring the pressure in the side hole. It was found that the piezoresistive pressure transducers could be conveniently assembled directly onto the hypodermic needles thus minimising ‘dead volume’ that would have affected the readings. Four-millimeter diameter side holes were used. In order to minimise the effect of the 20-mm aggregate, these were drilled to 40 mm deep with a 20-mm deep void space. Before applying the vacuum, three readings of pressure were taken at 10-s intervals in order to zero the pressure sensors.

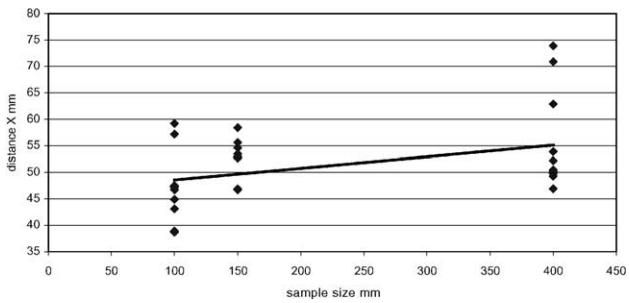

Fig. 8. Effect of sample size on distance X.

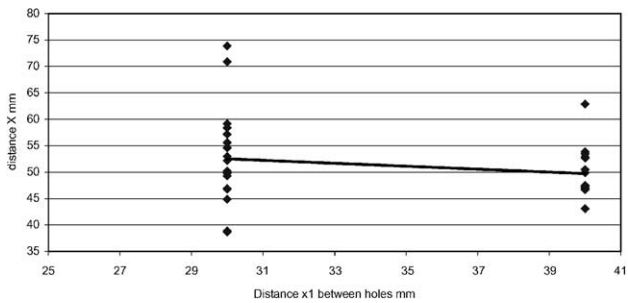

Fig. 9. Effect of distance between holes on distance X.

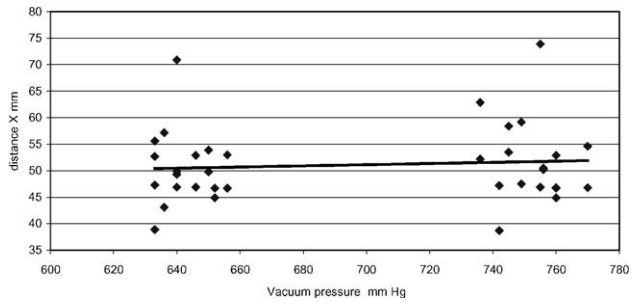

Fig. 10. Effect of vacuum pressure on distance *X*.

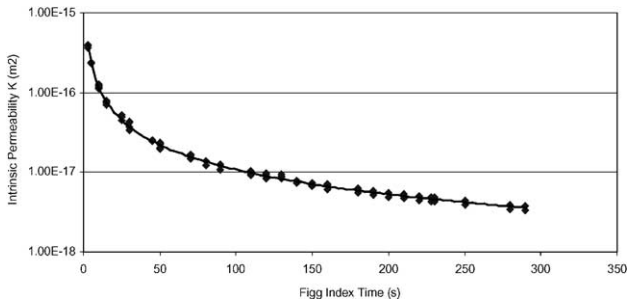

Fig. 12. Relationship between permeability and Figg index.

5.2. Results

For each concrete mix, the pressure values were measured for all the three holes. A typical graph of vacuum pressure against time is shown in Fig. 7. The distance *X* was derived by substituting the value of the applied constant vacuum pressure and the resulting vacuum pressure in the side holes in Eq. (6).

The distance *X* for each concrete studied is in Table 4 and plotted in Figs. 8–11 with regression lines to the data (where there are only two values of the dependant variable this becomes a line through the average values of *X*).

6. Discussion

It may be seen that this technique gives realistic values for the distance *X*. From Fig. 8, it may be seen that the distances lie within the specimen width, except the 100-mm cube specimen in cast number 3. The increase in specimen size shows a minor increase in *X* that was expected from the closeness of the radius *X* to the edge of the 100-mm cubes. The averages from the 150- and 400-mm samples are similar. The use of these larger samples gives confidence that the observed values of approximately 50 mm were not a product of edge effects. From Figs. 9 and 10, it may be seen that increasing the separation of the holes or the vacuum pressure only had a very minor effect on *X* giving confidence in the modelling method. Fig. 11 shows that there was very little change in *X* with w/c ratio. This does not indicate that the permeability did not change because a more permeable sample will have a higher rate of extraction of air from the side hole but it will also have a higher rate of replenishment.

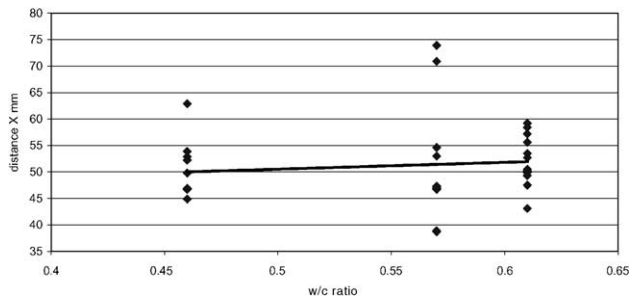

Fig. 11. Effect of w/c ratio on distance *X*.

The following method is proposed for testing concrete:

1. Prepare for the Figg test using the standard method but with an additional hole 4 mm in diameter, 40 mm deep at a distance of 30 mm from the centre hole.
2. Set up a data logger to take pressure readings in both holes at 10-s intervals.
3. Apply a constant vacuum to the centre hole until a stable pressure is recorded in the side hole and then seal the input and let the vacuum decay.
4. Calculate the distance *X* from Eq. (6) and then calculate the permeability by fitting Eq. (7) to the vacuum decay transient. This may be done by applying the equation at two different times and subtracting.

It may be seen that in this study the distance *X* was typically 50 mm. In order to calculate the permeability without drilling a second hole, this value might be used but all of the samples tested in this study had low moisture contents and a higher moisture content could reduce *X*. If the vacuum preconditioning [15] is used to standardise the moisture content, this would be unlikely to have any effect at less than 0.5 atm of vacuum, i.e., more than approximately 20 mm radius.

This method has been applied to a range of different samples and the permeability has been calculated [16]. Fig. 12 shows the results in which the permeability is plotted against the Figg permeability index, which is obtained directly from the transient. These show that this new method demonstrates the great changes in permeability indicated by small changes in Figg index time at short times.

7. Conclusions

1. A new test method, which is derived from the Figg test, is proposed, but uses additional holes drilled into the concrete. This new method reveals the volume of concrete that is being tested and permits calculation of the permeability.

2. Comparing various techniques has revealed that the method used for the standard Figg test is the best method to use for the measurement of pressure in small-diameter holes drilled into concrete samples.
3. The comparison of techniques has also given confidence in the results obtained for the pressure measurements.
4. The volume of concrete tested in the Figg test on a dry sample has a radius of approximately 50 mm. The test should therefore be reliable in concrete with 20-mm aggregate.
5. The new test shows the very large changes in permeability corresponding to small changes in the Figg index.

This new test is a modification of the original Figg test that was introduced in the early 1970s. There had been modifications to the original Figg test in order to improve its repeatability and sensitivity, which were not taken into account while carrying out the investigation reported in this paper. Therefore, the proposed test does not necessarily have improved repeatability and sensitivity compared to the modified Figg tests. The primary objective of this investigation was to obtain a coefficient of permeability from the original Figg test.

References

[1] J.H. Bungey, Environmental effects on surface measurements, Proceeding of the 3rd International Conference Bahrain Society of Engineers, Bahrain, 1989, pp. 443–457.
[2] A. Meyer, The importance of surface layer for durability of concrete structures, Am. Concr. Inst., SP 100 (1) (1987) 49–59.
[3] C.Z. Hong, L.J. Parrott, Air Permeability of Cover Concrete and the Effect of Curing, C&CA Services, British Cement Association, Crowthorne, Berkshire, UK, 1989 (October).
[4] P.A.M. Basheer, F.R. Montgomery, A.E. Long, The 'Autoclam permeability system' for measuring the in-situ permeation properties of concrete, International Conference on Non-Destructive Testing in Civil Engineering, Liverpool, 14–16 April, British Institute of Non-Destructive Testing, Northampton, 1993, pp. 235–260.
[5] F.R. Montgomery, P.A.M. Basheer, A.E. Long, A comparison between the Autoclam permeability system and the initial surface absorption test, Proceeding of International Conference on Structural Faults and Repair 93, vol. 3, Engineering Technics Press, Edinburgh, 1993, pp. 71–77.
[6] W.J. McCarter, M. Emerson, H. Ezirim, Properties of concrete in the cover zone: development in monitoring techniques, Mag. Concr. Res., (172) (1995) 243–251 (September).
[7] M.A. Wilson, S.C. Taylor, W.D. Hoff, The initial surface absorption test (ISAT): an analytical approach, Mag. Concr. Res. 50 (2) (1998) 179–185 (June).
[8] M. Levitt, Non-destructive testing of concrete by the initial surface absorption method, Proceeding of Symposium on Non-Destructive Testing of Concrete and Timber, Institute of Civil Engineers, London, 1969, pp. 23–36.
[9] J.W. Figg, Methods of measuring the air and water permeability of concrete, Mag. Concr. Res. 25 (85) (1973) 213–219 (December).
[10] R.K. Dhir, P.C. Hewlett, Y.N. Chan, Near-surface characteristics of concrete: assessment and development of in situ test methods, Mag. Concr. Res. 39 (141) (1987) 183–195 (December).
[11] P.A.M. Basheer, Clam Permeability Test for Assessing the Durability of Concrete, PhD thesis, Queens University, Belfast, 1991.
[12] P.A. Claisse, H.I. Elsayad, I.G. Shaaban, Test methods for measuring fluid transfer in cover concrete, ASCE Mater. J. 11 (2) (1999) 138–143 (May).
[13] J.M. Illston, Construction Materials, 2nd ed., E & FN Spon, London, 1994.
[14] BS 5075: Part 2, Specification for Air-Entraining Admixtures, BSI, London, 1982.
[15] P.A. Claisse, H.I. Elsayad, I.G. Shaaban, Absorption and sorptivity of cover concrete, ASCE Mater. J. 9 (3) (1997) 105–110 (August).
[16] T. Adham, The Development of a Test Procedure to Determine the Potential Durability of Concrete Structures, PhD thesis, Coventry University, 2001.